ANALYTICAL STUDY OF EXERGETIC EFFICIENCY OF A SOLAR AIR HEATER WITH C-SHAPE ROUGHNESS ELEMENT

Sureshkumar PETCHIMUTHU [1]* and Sathiya Moorthy RAJENDRAN [2]
[1]*Department of Mechanical Engineering,
Government College of Engineering, Tirunelveli 627-007, India
[2]Department of Mechanical Engineering
Anna University Regional Campus, Coimbatore 641-046, India
Corresponding author; E-mail: ppskumar200@gmail.com

This study analytically evaluates the exergetic efficiency of solar air heaters incorporating C-shaped rib roughened absorber plates. Compared to flat plate designs, the proposed geometry significantly enhances energy performance. Optimal roughness parameters for maximizing exergy efficiency are identified, providing design guidelines for improved solar air heater systems. The maximum value of exergy efficiency of the Solar air heater, with C-shaped ribs was obtained as 5.9%.
Keywords: *C-Shaped ribs, Exergy, Relative roughness pitch, Solar air heater, Relative roughness height, Analytical Study*

1. Introduction

Solar energy is the radiant light and heat from the Sun that can be harnessed using various technologies to generate electricity, provide heating, and support other energy needs. It is a renewable and sustainable energy source with minimal environmental impact. Solar collectors can be classed according to the type of working fluid utilized. There are three major types: (i) Air-based solar collectors use air to absorb and transport heat. (ii) Liquid-based solar collectors use liquids, usually water or antifreeze solutions, to gather and transmit thermal energy. (iii) Hybrid solar collectors use air and liquid systems to capture and transport solar energy more efficiently.
The following reason air based solar collectors used; Air is readily available and more economical as it doesn't need the same infrastructure as liquid-based systems. Unlike liquids, air doesn't freeze, so antifreeze solutions and maintenance issues in cold climates are not a concern. Air-based systems are also lighter, making installation and structural requirements simpler. A simple solar air heater (SAH) contains a rectangular cross-section duct that carries the air to be heated underneath a metallic absorber plate that has been blackened on one side to enhance solar energy absorption which incident on it. This air which is heated will be used for a number of functions, involving room drying and heating for industrial and agricultural reasons. Yadav and Gattani [1] found ways to improve heat transfer in a duct without significantly increasing friction by using different types of rough surfaces. Yadav and Gattani [2] this article reviews different ways to improve solar air heaters by using different types of ribs. Agrawal et al.[3], the impact of a double arc reverse-shaped plate by uniformly gapped was examined using experimental studies using the following parameters: duct aspect ratio *(W/H)*=8, *Re*=3000-14000, α =30^0, 45^0, 60^0, 75^0, relative roughness height (e/D_h) = 0.027, and relative roughness pitch (p/e)=10. The findings show that the highest rises in the *Nu* and *f* are 2.85 and 2.42 above a smooth plate, correspondingly. Dong et al.[4], this research focuses on the performance of flat-plate SAH with slanted groove ripple surfaces. The study investigates the impact of groove amplitude, angle of attack, and array number on overall performance in Reynolds number range between 12000 -24000. The inclined grooves improve pressure drop and heat transfer, while the ripple surface provides superior performance of thermo-hydraulic, with Nusselt values that are 1.04 to 1.94 times greater in comparison to smooth ducts. Mahanand and Senapati [5]**,** examined the effect of heat transfers and flow field analysis with transverse inverted-T-shaped ribs on solar air heaters. The author discovered 2.747, 3.404, and 1.86 times more improvements in Nusselt number, friction factor, as well as thermal enhancement

factor comparing to smooth plate solar air heater. Abdullah et al.[6], this research focus on the usage of turbulators as well as external mirrors in a single-pass SAH. Turbulators are made of aluminium cans, and exterior reflectors boost energy input. Three types of absorbent plates were tested: flat plates without cans, aligned cans, and staggered cans. A comparison was done between modified and regular SAHs. The study discovered that a staggered heater with external reflectors and guiding vanes had a maximum daily efficiency of 73.4% at 0.05 kg s^{-1}. Ghritlahre et al. [7], the survey examines the heat transmission and "thermal performance of arc-shaped roughened solar air heaters having an apex down and up airflow". Experiments that have varied mass flow rates revealed that thermal efficiency raised with mass flow rate. The apex-up configuration conducted 33.2 percent better in heat transmission than the apex-down arrangement, demonstrating that the apex-up configuration is more efficient. Noghrehabadi et al. [8] this study compares the thermal performance of square and rhombic flat plate solar collectors. Both designs exhibited similar efficiency at midday, but the rhombic collector outperformed the square collector in morning and afternoon conditions. Increasing flow rate improved efficiency for both designs, with the rhombic collector consistently demonstrating superior performance. Alfarawi et al. [9]**,** assessed the flow friction and Heat transfer experiments performed on a rectangular duct with *3* separate rib geometries such as hybrid ribs, semi-circular, and rectangular. Reynolds numbers that varied from 12,500-86,500, as well as rib pitch-to-height ratios varying from 6.6-53.3, were used in the experiment. The results showed that hybrid ribs had better heat transmission (Nu/Nu_s) and higher efficiency indices than semi-circular ribs and rectangular. Novel correlations were discovered for all analyzed geometries and configurations. Gill et al.[10], examined the influence of broken arc ribs, researchers discovered 2.37, 2.55, and 1.94 times more improvements in friction factor, Nusselt number, as well as the performance of thermo-hydraulic than smooth plate solar air heater. To optimize the duct properties on an arrangement of arc-shaped rib at SAH, Sahu and Prasad [11]**,** developed a mathematical model. At a Reynolds number of 15,000, a fixed pitch ratio of 10, a comparative roughness with the 0.0422 height, and a 0.3333 relative angle of attack, the highest exergy efficiency of 3.6 percent was attained. A SAH component with the shape of an arc protruding by the roughness element was the subject of an analytical analysis by Yadav et al. [12]**,** at various ranges of *Re*. It discovered that exergy effectiveness (2.2%) reached its highest at a $\Delta T/I$ of 0.02 $m^2K\ W^{-1}$, *P/e* of 12, e/D_h of 0.03, as well as α of 60^0. In this research by Yongsiri et al. [13], the transmission of heat and turbulent flow in a channel with inclined removable ribs are studied numerically. It analyses pressure loss, thermal performance, as well as heat transfer utilizing the finite volume method as well as the SIMPLE approach. The findings demonstrate that inclined ribs with 60^o and 120^o angles have increased thermal performance factors and heat transfer rates having high Reynolds numbers, but not at the low Reynolds numbers. Singh et al. [14], have conducted experimental research on the transfer of heat and friction in airflow in rectangular ducts having several arc-shaped ribs. Correlations were discovered for the factor of friction and the Nusselt number. Kumar et al. [15]**,** investigational study for transfer of heat and friction in air flow in an absorber with multi-v-shaped ribs the following parameters were as *Re* from the 2000-20,000, *P/e* values of 6 to12, *e/D* values of 0.022 to 0.043, *g/e* values of 0.5 to 1.5, *Gd/L* values of 0.24-0.80, *W/w* values of 1 to 10 and an angle of attack of 30 to 75^0 were used. Findings show that the highest improvement in *Nu* of 6.74 and *f* of 6.37 times more than a smooth plate. . Lanjewar et al.[16], conducted a study on the features of heat transfer as well as the friction factor inside a rectangular duct having W-shaped ribs on its bottom and one large wall orientated at an angle with regard to the flow direction**.** The results exhibit that at an attack angle of 60^0, the largest increases in Nu = 2.36 and f = 2.01 are times compared to that of a smooth plate, respectively. Hans et al.[17], this research explores the influence of various v-rib roughness on the coefficient of heat transfer as well as the friction factor in synthetically roughened ducts. Numerous tests were run to gather information for the properties of fluid flow and heat transfer and correlations between the factor of friction and Nusselt number were established using the flow parameters and roughness geometry. Gupta and Kaushik [18]**,** examined the effectiveness, energy, along with energy performance assessment of solar air heater ducts equipped with various artificial roughness geometries The influence of V-shaped rib's geometrical parameters on the transmission of heat and properties of

the fluid flow for the solar air heater was experimentally examined by Ebrahim Momin et al.[19]**.** The investigation comprised a range of Reynolds numbers (*Re*) from 2500 to 18000, relative roughness heights (e/D_h) from 0.02-0.034, and flow angle of attack ranging to 30–90^0 with a fixed relative pitch of 10". When compared to a smooth absorber, it was discovered to have better heat transmission performance. In the current work, analytical modeling employing various heat or energy equations was used to determine the exergetic performance of both roughened and smooth solar air heaters. This study analytically evaluates the exergetic efficiency. The research aims to develop strategies for improving the efficiency of solar air heating systems while minimizing costs and maintaining a high-quality output. Compared to other rib configurations, such as rectangular or trapezoidal ribs, the C-shaped rib may offer the advantage of lower pressure drop. The C-shaped rib configuration can induce strong vortices and turbulence in the boundary layer flow. This enhanced turbulence promotes better mixing and heat transfer amid the fluid and the solid surface, leading to improved convective heat transfer coefficients. The streamlined shape of the C-rib could help minimize flow resistance while still effectively enhancing heat transfer. In conclusion, the study of solar air heaters with C-shaped ribs has the potential to make significant contributions to a wide range of fields. By understanding the effects of turbulence and heat transfer enhancement, researchers can improve the design and performance of various thermal systems, leading to more efficient and sustainable technologies. Researchers have looked at a wide variety of roughness element forms and sizes, but none have made an effort to test the effects of the current geometry. For roughened SAHs, an optimal value of several roughness parameters was found based on exergetic performance.

2. Solar Air Heater Performance Analysis

2.1 Thermal Analysis

The effectiveness of a SAH is described as the ratio of heat amount gathered from the sun to the radiation amount that hits the surface of collector. Rib placements above the absorber are shown in Figure 1.

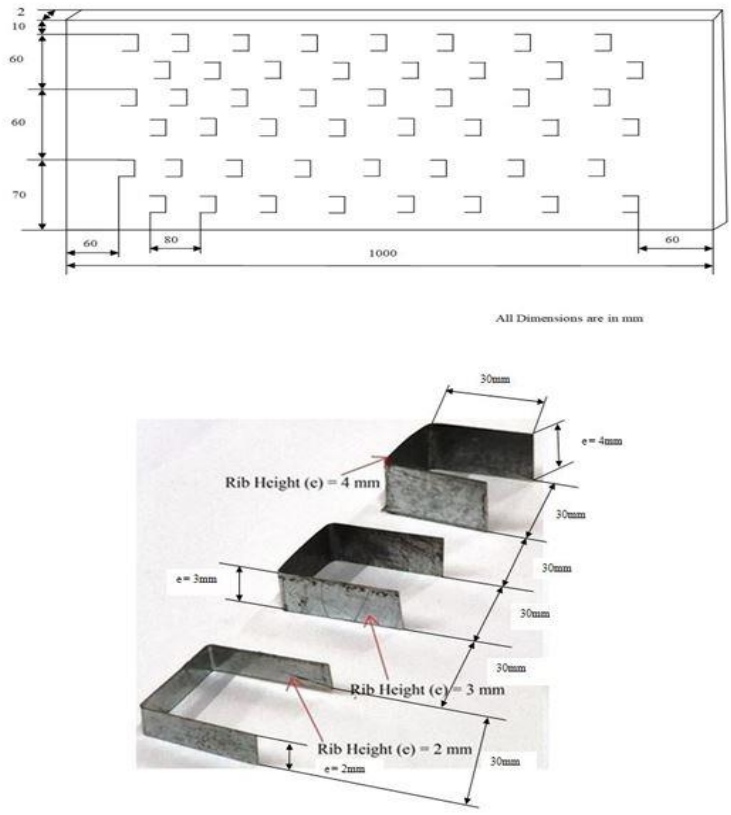

Fig. 1. Rib positions over the absorber plate

The thermal efficiency of SAH is computed from **Eq. (1).**

$$\eta_{th} = \frac{mC_P(T_0 - T_i)}{IA_c} \quad \textbf{(1)}$$

Where: m [kgs^{-1}] is the mass flow rate of the working fluid, C_p [$J\ kg^{-1}K^{-1}$] is the specific heat, T_i [K] is the inlet temperature of the working fluid, T_o [K] is the Outlet temperature of the working fluid, I [Wm^{-2}] is the solar radiation intensity and A_c [m^2] is the surface area of the absorber.

The thermal efficacy of SAH in terms of heat removal factor by **Eq. (1)**, [17]:

$$\eta_{th} = \frac{Q_u}{IA_c} = F_R\left[(\tau\alpha)_e - U_L\left(\frac{T_i - T_a}{I}\right)\right] \quad \textbf{(2)}$$

Where: Q_u [W] is the useful heat gain**,** F_R [–] is the collector heat removal factor**,** τα [-] is the transmissivity – absorptivity product of glass cover= 0.85**,** U_L [$Wm^{-2}\ K^{-1}$] is the overall heat loss coefficient and T_a [K] is the ambient temperature.

2.2 Exergy Analysis

It is a technique that is effective for assessing the complete effectiveness of solar systems, such as SAHs.

Exergetic efficiency (η_{EX}) is assessed by **Eq. (3)** as stated by Altfeld et al., [18].

$$\eta_{EX} = \frac{E_n}{E_s} \quad \textbf{(3)}$$

The flow of net exergy (E_n) is evaluated with **Eq. (4)**.

$$E_n = IA_c\eta_{th}\eta_c - P_m(1 - \eta_c) \quad \textbf{(4)}$$

Where: $\eta_c = \left(1 - \frac{T_a}{T_f}\right)$, P_m [W] is the pumping power and T_f [K] is the average temperature of air

Exergy inflow is calculated from **Eq. (5).**

$$E_s = A_c\left[1 - \frac{T_a}{T_{sun}}\right] \quad \textbf{(5)}$$

Where: T_{sun} [K] is the sun temperature.

Exergy efficiency may be maximized by reducing losses in exergy and increasing the net flow of exergy. Exergy Losses are made up of the following components [18].

(i) Exergy is lost because of friction by **Eq. (6).**

$$E_{L\Delta P} = m\,\Delta P\left(\frac{T_a}{\rho_a T_f}\right) \quad \textbf{(6)}$$

Where: ΔP [Pa] is the pressure difference and ρ_a [kgm^{-3}] is the Density of air.

(ii) Exergy loss owing to radiation &convection transferring of heat by the absorber to surroundings by **Eq. (7).**

$$E_{EN} = U_L A_C (T_p - T_a)\left(1 - \frac{T_a}{T_p}\right) \quad \textbf{(7)}$$

Where: T_p [K] is the average temperature of absorber plate.

(iii) Exergy is lost as a result of the absorber plate absorbing radiation by **Eq. (8).**

$$E_{LI} = I\,A_C\,(\tau\alpha)_e\left(\eta_{ex} - \left(1 - \frac{T_a}{T_p}\right)\right) \quad \textbf{(8)}$$

(iv) Exergy Loss because ofheat transfer toa working fluid by **Eq. (9).**

$$E_{L\Delta F} = U_L A_C \eta_{th}\ \left(\frac{T_a}{T_f} - \frac{T_a}{T_p}\right) \quad \textbf{(9)}$$

(v) Optical exergy loss by **Eq. (10).**

$$E_{LO} = IA_C\ \eta_{ex}\ (1 - (\tau\alpha)_e) \quad \textbf{(10)}$$

3. Analytical study

The thermal performance of a roughened SAH is similar to that of flat plate SAH, as in both the SAH radiation is absorbed by absorber plate and collected heat is transferred to the working fluid. It may be noted that since the objective of this work is to present a methodology for optimum design of the solar air heater. Since the working fluid is air, Density, Specific heat, Thermal conductivity and Dynamic viscosity are 1.225 Kgm^{-3}, 1006 $Jkg^{-1}K^{-1}$, 0.0262 $Wm^{-1}K^{-1}$, 1.81 × 10-5 $Kgm^{-1}s^{-1}$, respectively. The study included Re from 3000 to 18000, e/D from 0.025 to 0.05, P/e from 10 to 20. Figure. 2. Shows calculation steps involved in analyzing a solar air heater system.

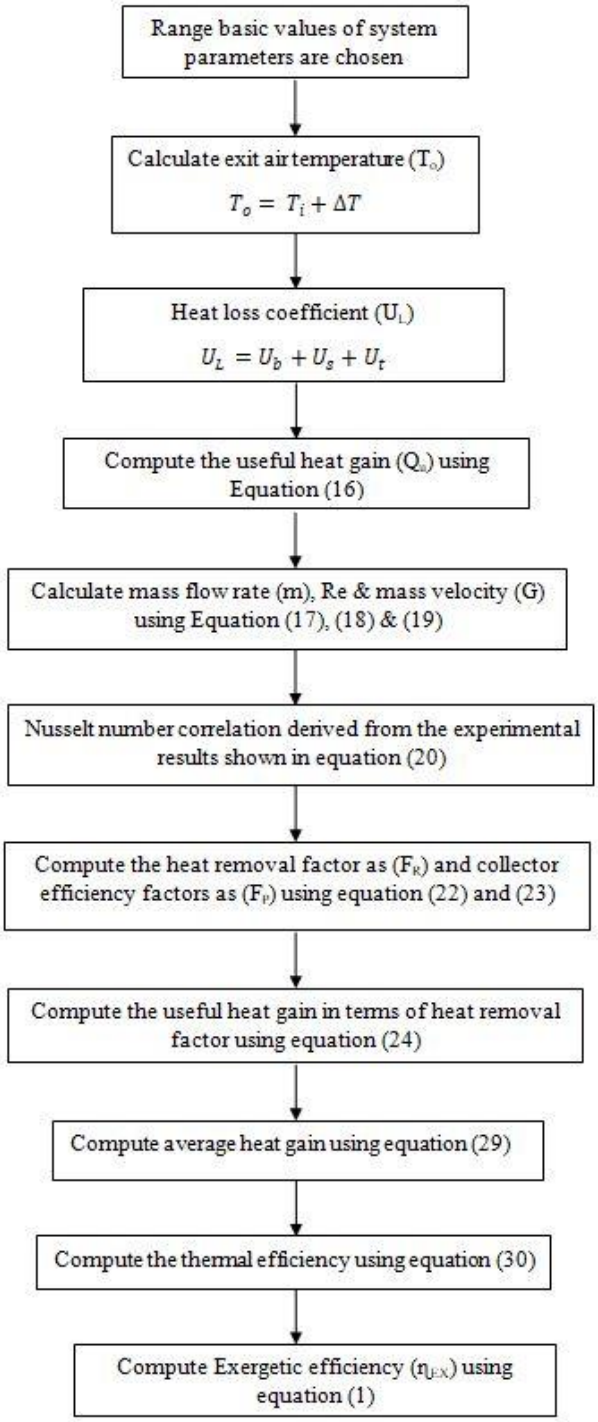

Fig. 2. Calculation steps involved in analyzing a solar air heater system

Outlet temperature is calculated from **Eq. (11)**.

$$T_o = T_i + \Delta T \quad \textbf{(11)}$$

Where: T_0 [K] is the Outlet temperature of the working fluid, $T_i = T_a$ [K] is the ambient temperature of the working fluid and ΔT [K] is the Temperature difference in working fluid.

Complete heat loss coefficient is denoted by U_L is calculated by the **Eq. (12)**.

$$U_L = U_b + U_s + U_t \quad \textbf{(12)}$$

Where: U_L [$Wm^{-2}K^{-1}$] is the heat loss coefficient of the absorber, U_b [$Wm^{-2}K^{-1}$] is the back heat loss coefficient of the absorber, U_s [$Wm^{-2}K^{-1}$] is the edge heat loss coefficient of the absorber and U_t [$Wm^{-2}K^{-1}$] is the top loss coefficient of the absorber.

The relation shown below is utilized to compute the back heat loss coefficient U_b.

$$U_b = \frac{K_i}{\delta_i} \quad \textbf{(13)}$$

Where: k_i [$Wm^{-1}k^{-1}$] is the thermal conductivity of insulation and δ_i [m] is the thickness of insulation.

The relation shown below is utilized to compute the edge heat loss coefficient U_S.

$$U_S = \frac{(L+W)HK_i}{LW\delta_i} \quad \textbf{(14)}$$

Where: L [m] is the Collector length, W [m] is the Duct width and H [m] is the Duct height

The relation shown below is used to compute the top loss coefficient U_t Akhtar, Mullick, [19].

$$U_t = \left[\frac{M}{\left(\frac{C}{T_p}\right)\left(\frac{Tp-Ta}{M+f'}\right)^{0.252}} + \frac{1}{h_w}\right]^{-1} + \left[\frac{\sigma\left(T_p^2+T_a^2\right)(T_p+T_a)}{\frac{1}{\varepsilon p+0.0425M(1-\varepsilon_p)}+\frac{2M+f'-1}{\varepsilon_g}-M}\right] \quad \textbf{(15)}$$

Where: T_p [K] is the average temperature of absorber plate, T_a [K] is the average temperature of air, ε_p [-] is the absorber plate emissivity, ε_g [-] is the glass cover emissivity and V_w [ms^{-1}] is the velocity of the air.

$$f' = \left(\left(\frac{9}{h_w}\right) - \left(\frac{30}{h_w^2}\right)\right)\left(\frac{T_a}{316.9}\right)(1 + 0.091M)$$

$$h_w = 5.7 + 3.8V_w$$

$$C = 204.429\left(\frac{(cos\beta)^{0.252}}{L_1^{0.24}}\right)$$

ε_p = Absorber plate emissivity = 0.9

ε_g = Glass cover emissivity = 0.88

The relation shown below is used to compute the Initial mean plate temperature

$$T_P = \frac{T_0 + T_i}{2} + 10^0 C$$

The relation shown below is utilized to compute the useful heat gain

$$Qu_1 = \left[I(\tau\alpha)_e - U_L\left(T_p - T_a\right)\right]A_c \quad \textbf{(16)}$$

The relation shown below is utilized to calculate mass flow rate (m), Re and mass velocity (G).

$$m = \frac{Qu_1}{C_p\Delta T} \quad \textbf{(17)}$$

$$G = \frac{m}{WH} \quad \textbf{(18)}$$

$$Re = \frac{GD}{\mu} \quad \textbf{(19)}$$

Where: C_p [J kg^{-1} K^{-1}] is the specific heat of air, m [kg s^{-1}] is the mass flow rate of air and μ [N s m^{-2}] is the dynamic viscosity of air.

The correlation derived from the experimental results (using regression analysis), as shown below, is utilized to find the Nusselt number.

$Nu =$

$$4.9 \times 10^{-4} Re^{1.21} \left(\frac{P}{e}\right)^{3.2} \times \left[exp(-2.02)\left(log\left(\frac{P}{e}\right)\right)^2\right] \times \left(\frac{e}{D}\right)^{0.034} \times \left[exp(-1.29)\left(log\left(\frac{e}{D}\right)\right)^2\right] \textbf{(20)}$$

The relation shown below is utilized to compute the convective heat transfer coefficient (h)

$$h = \frac{Nu\,K}{D} \quad \textbf{(21)}$$

Where: k [W m^{-1} K^{-1}] is the thermal conductivity and D [m] is the hydraulic diameter of the duct.

The relation shown below is used to compute the heat removal factor as (F_R) and collector efficiency factors as (F_P)

$$F_P = \frac{h}{h+U_L} \quad \textbf{(22)}$$

$$F_R = \frac{mC_P}{U_L A_C}\left[exp\left(\frac{U_L A_C F_P}{mC_P}\right) - 1\right] \quad \textbf{(23)}$$

The relation shown below is used to compute the useful heat gain (Qu_2)

$$Qu_2 = F_R A_C \left[I(\tau\alpha)_e - U_L\left(\frac{T_0 - T_i}{2}\right)\right] \quad \textbf{(24)}$$

The valuable heat gain $Qu_1$and Qu_2 values are compared. Qu_1 =Qu_2. If Qu_1–Qu_2> 0.1% of the Qu_1 after that temperature of the plate is computed by using equation **(20)**.

$$T_P = T_a + \left[\frac{I(\tau\alpha)_e - \frac{Qu_2}{A_C}}{U_L}\right] \quad \textbf{(25)}$$

The correlation derived from the experimental results (using regression analysis), as shown below, is used to determine the friction factor.

$$f = 0.634 Re^{-0.419}\left(\frac{P}{e}\right)^{-0.456} \times \left[exp(0.052)\left(log\left(\frac{P}{e}\right)\right)^2\right] \times \left(\frac{e}{D}\right)^{-0.0211} \times \left[exp(0.834)\left(log\left(\frac{e}{D}\right)\right)^2\right] \textbf{(26)}$$

The relation shown below was utilized to compute the pressure drop (ΔP) in the duct

$$\Delta P = \frac{2fLV^2\rho_a}{D} \quad \textbf{(27)}$$

Where: f [-] is the friction factor and ρ_a [kg m-3] is the density of the air.

The relation shown below is used to compute the mechanical power (P_m)

$$P_m = \frac{m\Delta P}{\rho_a} \quad \textbf{(28)}$$

The average heat gain has been calculated by the average of Qu_1 and Qu_2

$$Qu = \frac{Qu_1 + Qu_2}{2} \quad \textbf{(29)}$$

The relation shown below is used to compute the thermal efficiency

$$\eta_{th} = \frac{Qu}{IA_C} \quad \textbf{(30)}$$

The Exergetic efficiency (η_{EX}) is assessed by **Eq. (1)**.

The same approach is used to compute the "exergetic efficiency" of the next combination of roughness parameters.

4. Results & Discussion

4.1 Exergetic Efficiency

Figure 3 depicts the change in exergetic efficiency as the function of Re and temperature rise parameter (TRP) for a SAH with C-shaped ribs and relative roughness heights of 0.025, 0.0375,

and 0.05, correspondingly, and a smooth absorber. The exergetic efficiency increases within the Re up to 6000, after which it starts to decrease all relative roughness heights and smooth absorbers. Exergetic efficiency values are low after the Reynolds number values are 6000. At lower Reynolds numbers, the flow is typically laminar or transitional, leading to lower frictional losses compared to turbulent flow at higher Reynolds numbers. Reduced frictional losses mean less exergy destruction due to fluid friction. Lower Reynolds numbers imply less turbulence, which can reduce mixing and potentially lead to lower entropy generation. Lower entropy generation is linked to higher exergetic efficiency. While higher Reynolds numbers enhance heat transfer, they also result in increased fluid friction due to increased turbulence. This increased pressure drop translates to higher pumping power requirements, reducing the overall system efficiency. The increased fluid friction and turbulence lead to higher entropy generation, which represents an irreversible loss of exergy. This exergy destruction offsets the gains in heat transfer, causing a decline in exergetic efficiency. The reason owing to considerable exergy loss from solar rays absorption by the absorber. The net exergy flow (En) to energy influx ratio is known as the exergetic efficiency (E_S). In addition, net exergy flow (En) is directly proportional to the exergetic efficiency. The variation between the heat energy captured and the power of pumping is known as net exergy flow. When the exergy of heat energy acquired at higher Reynolds numbers exceeds the exergy required for pump operation, the net exergy flow turns out to be negative. It causes exergetic efficiency declines with increases in Re. The results depicts in Fig. 4, for TRP < 0.025 K m^2W^{-1}, the smooth solar air heater has the maximum exergetic efficiency, whereas, for TRP > 0.025 K m^2W^{-1}, the protruded geometry with e/D=0.05 has the greatest exergetic efficiency. The value of TRP is different values for different Re and e/D. TRP values are 0.0220, 0.0261, 0.0357, 0.052 and 0.0632. At low TRP, the heat transfer from the absorber plate to the air is relatively low. A smooth surface might minimize thermal and fluid flow resistances, leading to lower exergy losses. By reducing irreversibilities, the smooth SAH can convert a higher proportion of the solar energy into useful work, resulting in higher exergetic efficiency. At higher TRP, the temperature difference between the absorber and air increases, driving more heat transfer. The protruded geometry with e/D=0.025, 0.0375 and 0.05 likely induces turbulence in the airflow, enhancing heat transfer and mixing. Improved heat transfer can lead to a higher outlet air temperature, increasing the exergy efficiency of the air. The inlet air passes through between the c- shaped ribs i.e., three sides of the c-shaped ribs cause more turbulent flow and flow separation compared to other shapes of ribs. The flow separation will generate a vortex. This phenomenon increases the heat absorption between ribs and the flowing air. This is because of protrusion's enhanced ability to conduct heat because of flow separation, vortex production at both sides of the protrusion, and main flow impingement. Due to the obstacle the protrusions create, when the main flow impacts the front side of them, a vortex forms Bhushan, Singh, [20].

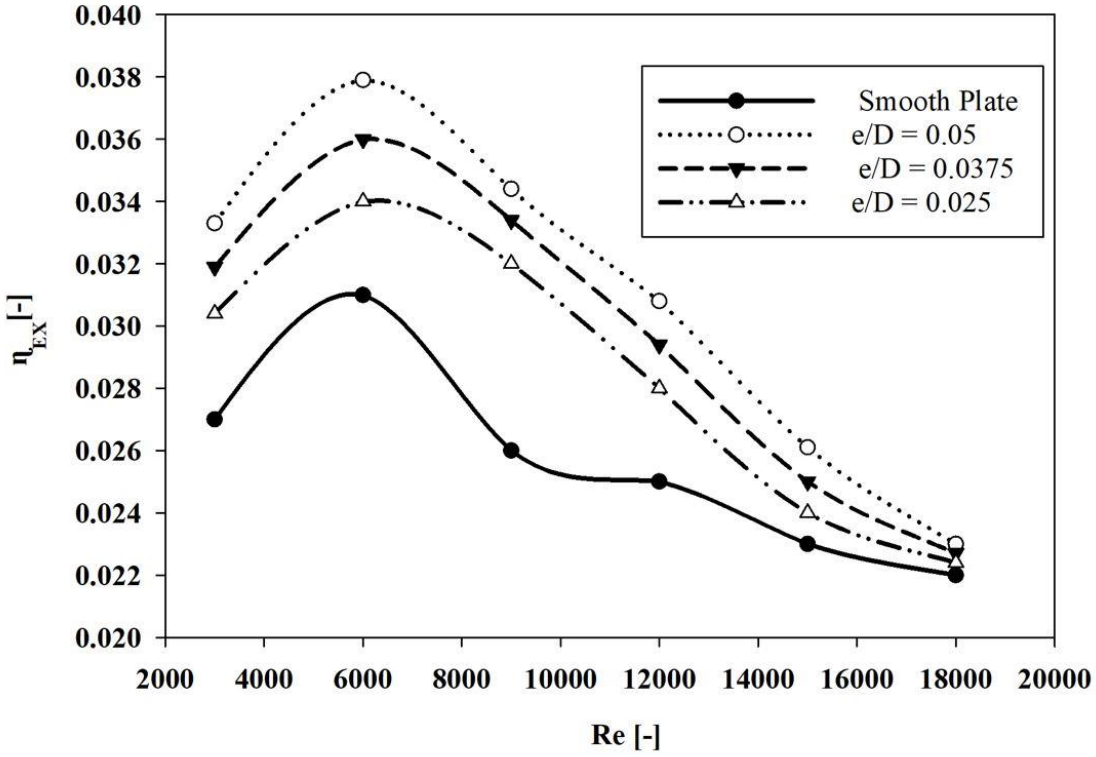

Fig. 3. Variation of Exergetic efficiency along Re for various (e/D)

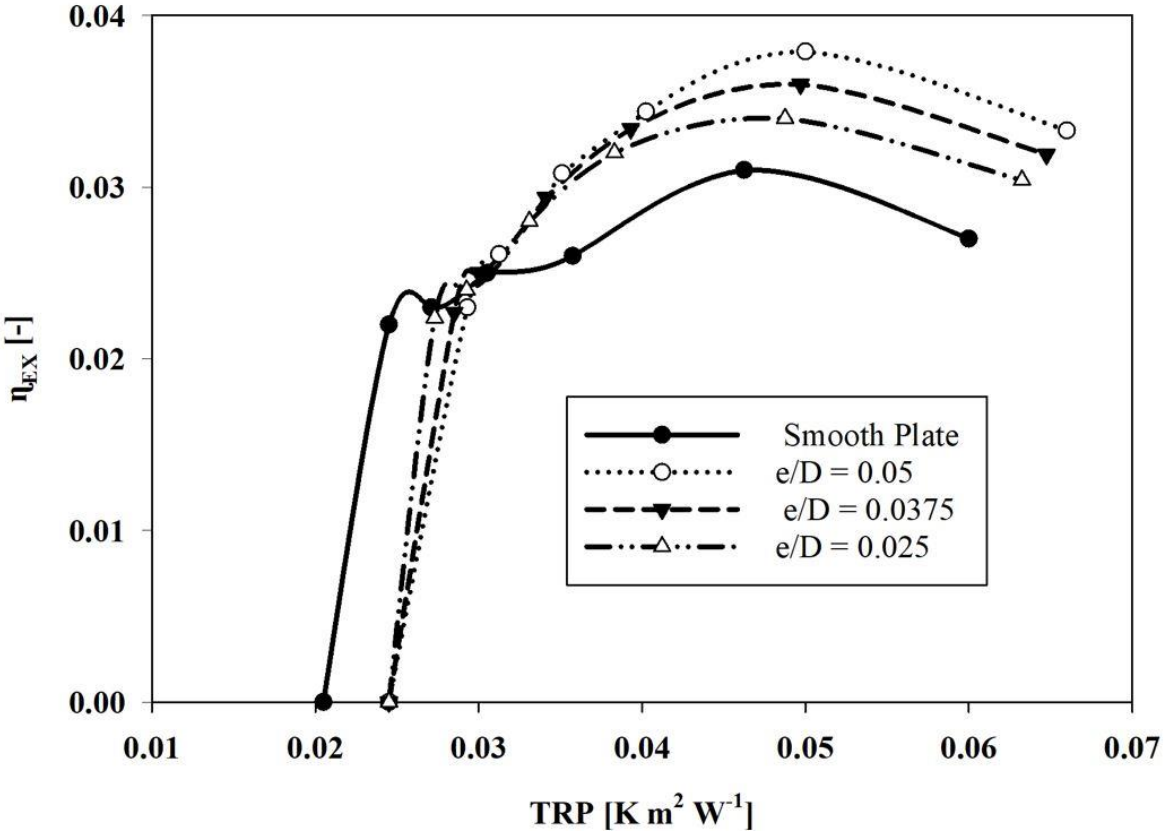

Fig. 4. Variation of Exergetic efficiency along TRP for various (e/D)

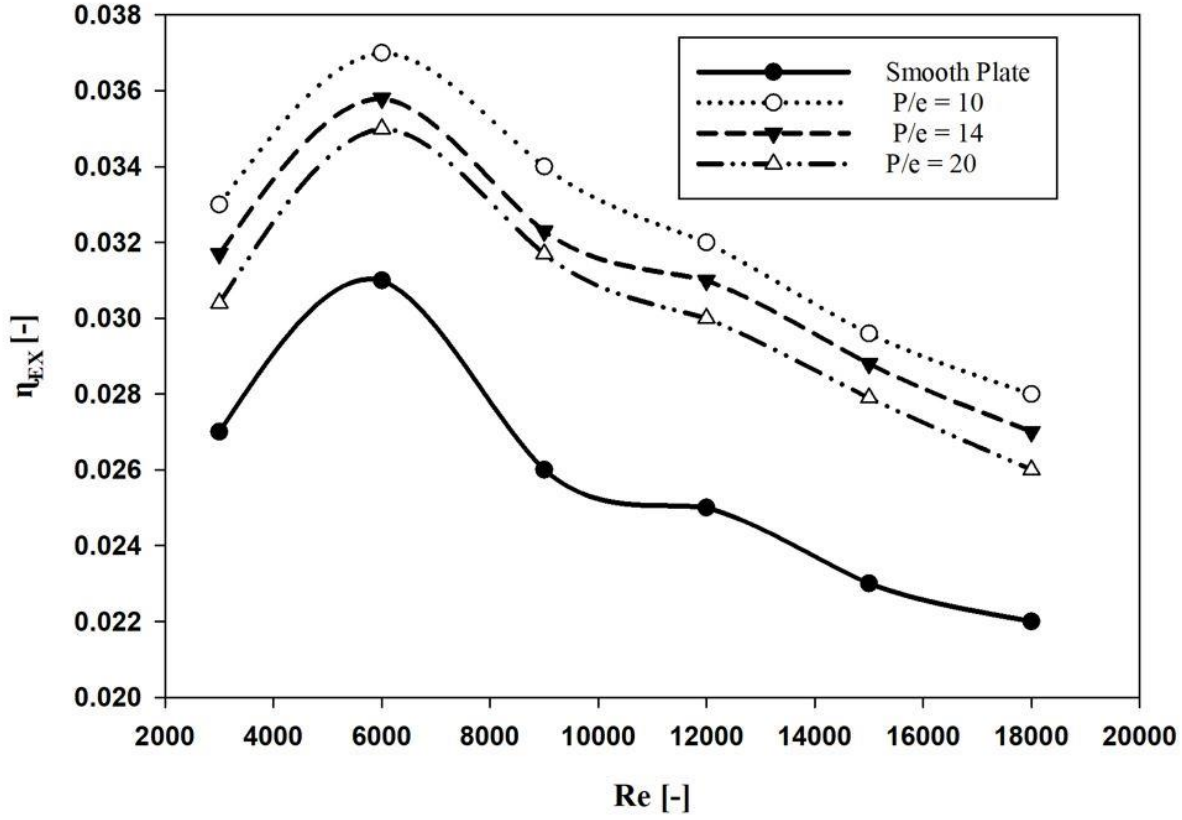

Fig. 5. Variation of Exergetic efficiency along Re for various (P/e)

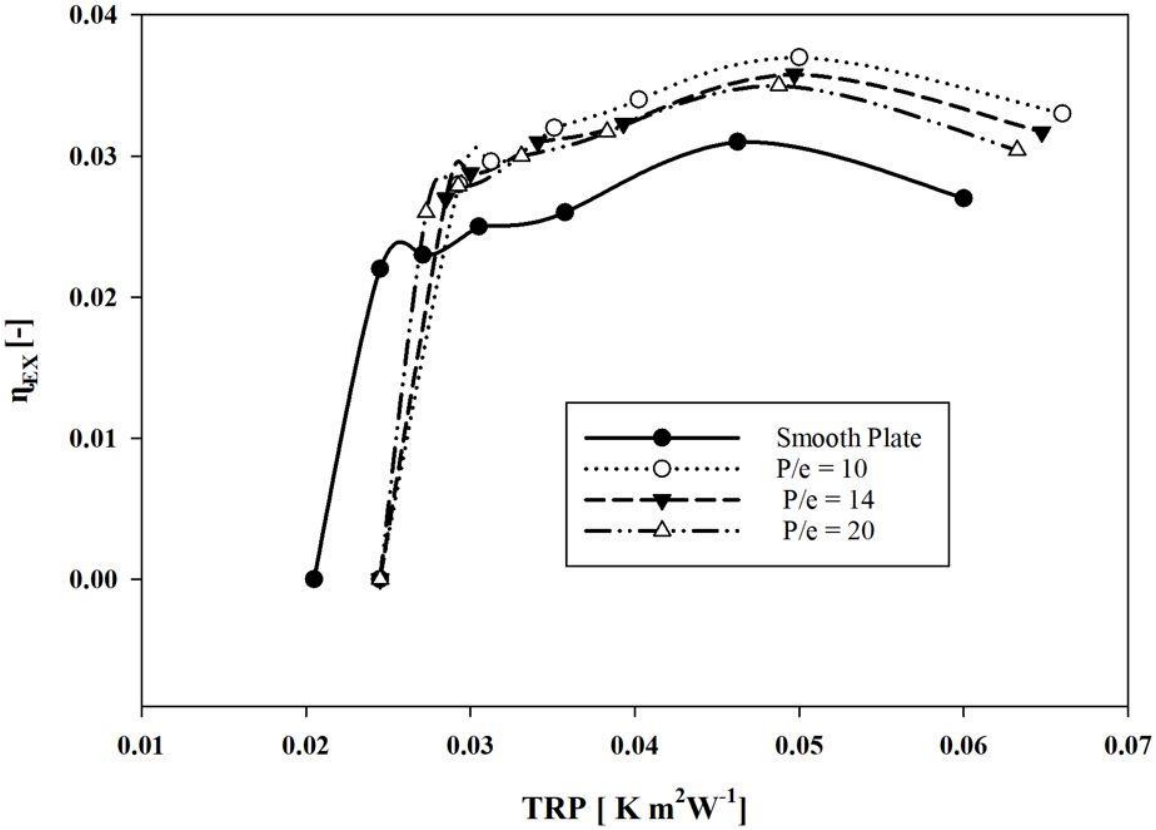

Fig. 6. Variation of Exergetic efficiency along TRP for various (P/e)

In accordance with Fig. 5, the best exergetic efficiency is reached at P/e = 10 for Re>20,500, and Re<20,000, for smooth solar air heater, which leads to higher exergetic effectiveness than the

extended roughness geometry, and Figure 6 represents the exergetic efficiency as a function of the TRP for a variety of relative roughness pitch (p/e) (Yadav et al., 2014). It can be shown that the p/e of 10 gives the exergetic efficiency the highest value for TRP values greater than 0.025 K m^2W^{-1}. This is a result of the absorber plate forming the greatest numbers for reattachment points over the absorber per unit length and augmentation in heat transmission takes place, the Nusselt number and the exergetic efficiency become maximum. The wake zone before and behind the ribs combining will remains stagnant at that place which reduces the transfer of heat and causes a heat transfer coefficient low value and low exergetic efficiency. Similarly, the P/e value less compared to the optimal value does not enable the free shear layer to reattach among successive ribs. Similar to this, relative roughness pitch values over the ideal reduce the numbers for reattachment points absorber surface unit length, decreasing the "heat transfer coefficient" and exergetic efficiency.

4.2 Design plot for extended roughness parameters

Figures 7 and 8 illustrate plots of optimal values of "relative roughness height" (e/D) and "relative roughness pitch"(P/e) that associate with the greatest exergetic efficiency for certain values of TRP. Figure 6 displays the P/e values plot related to the highest exergetic efficiency for various TRP. As can be shown, for all solar irradiation levels, the (P/e) = 10 is the optimal value of the TRP>0.04 K $m^2W^{-1}$and the P/e=20 is the optimal value for TRP<0.019 K m^2W^{-1}. Fig. 7 shows that for all insolation values, the e/D of 0.05 is the optimal value for TRP>0.03 K $m^2W^{-1}$and the e/D of 0.025 is the optimum value for TRP<0.018 K m^2W^{-1}. The optimal value of e/D is a function of solar radiation and TRP for values ranging from 0.01 to 0.060.

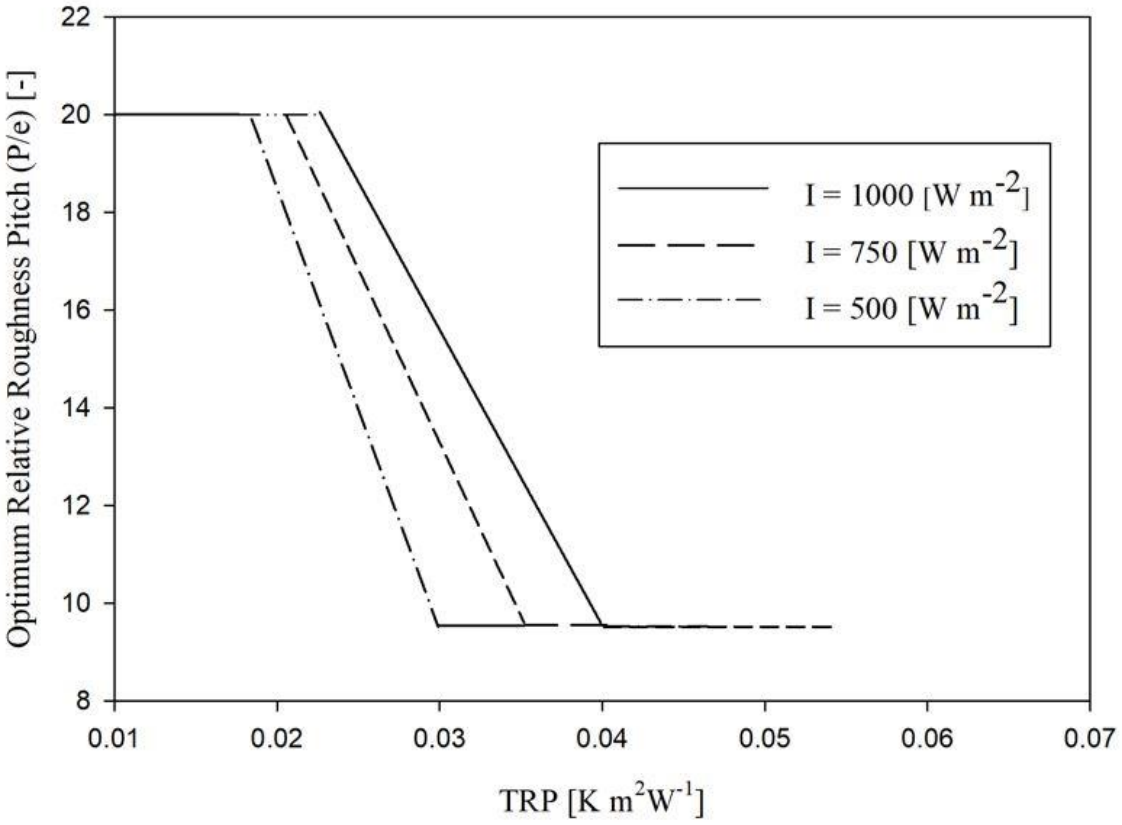

Fig. 7.Optimum values of P/e based on exergetic efficiency criterion.

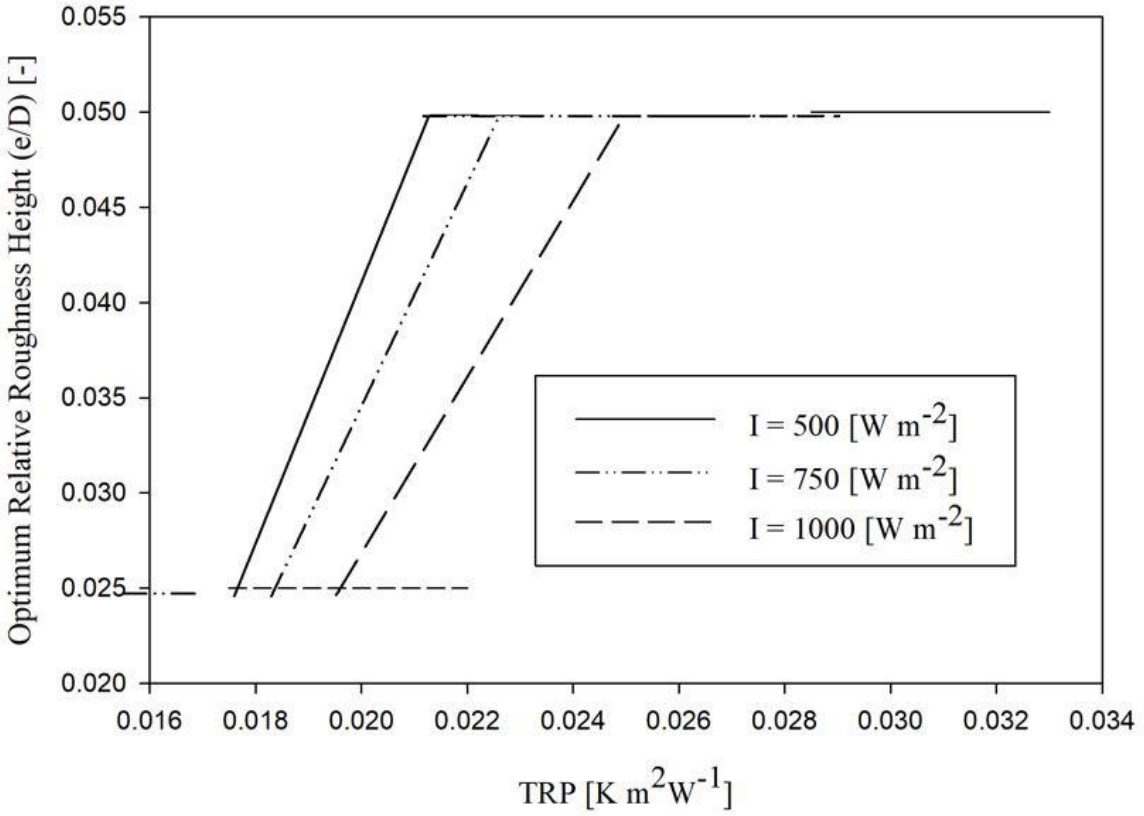

Fig. 8. Optimum values of e/D based on exergetic efficiency criterion

5. Conclusion

Based on the exergetic efficiency of the C-shaped rib roughened SAH, this analytical research suggests a mathematical model for forecasting its performance. Under the same working conditions, the outcomes obtained were compared to flat SAHs. The following findings are reached:

(i) The exergetic efficiency of SAHs using c-shaped rib roughened absorber plates has increased significantly. The exergetic efficiency improves by up to 26.6% in comparison to flat plate SAH.

(ii) With a growing Reynolds number (Re), exergetic efficiency rises, reaches a maximum, and then declines as Reynolds number rises. When Re is less than 20,000, e/D is 0.05, and P/e is 10, a c-shaped roughened SAH performs most efficiently in terms of energy. To raise the amount of energy extracted from the system, it is thus advisable to run the SAH or another solar system that lies at this range. A roughened solar air heater loses exergetic efficiency over 20,000, making it unpleasant to use the SAH above this Reynolds number.

(iii) The flow Reynold's number as well as roughness parameters have a significant impact on exergetic efficiency. The optimum set of roughness parameters is uniform for all radiation values. The optimum roughness parameter is e/D = 0.05 and p/e = 10.

(iv) The current exergetic efficiency requirements for solar thermal system analysis are appropriate for designing roughened SAHs, and the design plots may be utilized to construct c-shaped rib roughened SAHs.

(v) Combine SAHs with thermal energy storage systems to provide continuous heat supply and improve overall system efficiency.

(vi) There is tremendous scope for future study of C shaped roughened solar air heater with thermal energy storage systems to provide continuous heat supply and improve overall system efficiency.

References

[1] Yadav, A. S., Gattani, A., Revisiting the influence of artificial roughness shapes on heat transfer enhancement, *Materials Today: Proceedings*, *62* (2022), 3, pp. 1383-1391, https://doi.org/10.1016/j.matpr.2021.12.254

[2] Yadav, A. S., Gattani, A., Solar thermal air heater for sustainable development, *Materials Today: Proceedings*, *60* (2022), 1, pp. 80-86, https://doi.org/10.1016/j.matpr.2021.11.630

[3] Agrawal, Y., et. al., Enhancement Of Thermo-Hydraulic Performance Using Double Arc Reverse Ribs In A Solar Collector: Experimental Approach, *Materials Today: Proceedings*, *47* (2021), pp.6067–6073, https://doi.org/10.1016/j.matpr.2021.04.623

[4] Dong, Z., et. al., A Study On Heat Transfer Enhancement For Solar Air Heaters With Ripple Surface, *Renewable Energy*, *172* (2021), pp.477–487, https://doi.org/10.1016/j.renene.2021.03.042

[5] Mahanand, Y., Senapati, J. R., Thermal Enhancement Study Of A Transverse Inverted-T Shaped Ribbed Solar Air Heater, *International Communications in Heat and Mass Transfer*, *119* (2020), 104922, https://doi.org/10.1016/j.icheatmasstransfer.2020.104922

[6] Abdullah, A. S., et. al., Experimental Investigation Of Single Pass Solar Air Heater With Reflectors And Turbulators, *Alexandria Engineering Journal*, *59* (2020), 2, pp.579–587, https://doi.org/10.1016/j.aej.2020.02.004

[7] Ghritlahre, H. K., et. al., Thermal Performance And Heat Transfer Analysis Of Arc Shaped Roughened Solar Air Heater – An Experimental Study, *Solar Energy*, *199* (2019), pp.173–182, https://doi.org/10.1016/j.solener.2020.01.068

[8] Noghrehabadi, A., et. al., An Experimental Study Of The Thermal Performance Of The Square And Rhombic Solar Collectors, *Thermal Science*, *22* (2018), 1, pp. 487-494, DOI: 10.2298/TSCI151228252N

[9] Alfarawi, S., et. al., Experimental Investigations Of Heat Transfer Enhancement From Rectangular Duct Roughened By Hybrid Ribs, *International Journal of Thermal Sciences*, *118* (2017), pp.123–138 https://doi.org/10.1016/j.ijthermalsci.2017.04.017

[10] Gill, R. S., et. al., Investigation On Performance Enhancement Due To Staggered Piece In A Broken Arc Rib Roughened Solar Air Heater Duct, *Renewable Energy*, *104* (2017), pp.148–162, https://doi.org/10.1016/j.renene.2016.12.002

[11] Sahu, M. K., Prasad, R. K., Exergy Based Performance Evaluation Of Solar Air Heater With Arc-Shaped Wire Roughened Absorber Plate, *Renewable Energy*, *96* (2016), pp.233–243, https://doi.org/10.1016/j.renene.2016.04.083

[12] Yadav, S., et. al., Exergetic Performance Evaluation Of Solar Air Heater Having Arc Shape Oriented Protrusions As Roughness Element, *Solar Energy*, *105* (2014), pp.181–189, https://doi.org/10.1016/j.solener.2014.04.001

[13] Yongsiri, K., et. al., Augmented Heat Transfer In A Turbulent Channel Flow With Inclined Detached-Ribs, *Case Studies in Thermal Engineering*, *3* (2014), pp.1–10, https://doi.org/10.1016/j.csite.2013.12.003

[14] Singh, A. P., et. al., Heat Transfer And Friction Factor Correlations For Multiple Arc Shape Roughness Elements On The Absorber Plate Used In Solar Air Heaters, *Experimental Thermal and Fluid Science*, *54* (2014), pp.117–126, https://doi.org/10.1016/j.expthermflusci.2014.02.004

[15] Kumar, A., et. al., Development Of Correlations For Nusselt Number And Friction Factor For Solar Air Heater With Roughened Duct Having Multi V-Shaped With Gap Rib As Artificial Roughness, *Renewable Energy*, *58* (2013), pp.151–163, https://doi.org/10.1016/j.renene.2013.03.013

[16] Lanjewar, A., et. al., Experimental Study Of Augmented Heat Transfer And Friction In Solar Air Heater With Different Orientations Of W-Rib Roughness, *Experimental Thermal and Fluid Science*, *35* (2011), 6, pp.986–995, https://doi.org/10.1016/j.expthermflusci.2011.01.019

[17] Hans, V. S., et. al., Heat Transfer And Friction Factor Correlations For A Solar Air Heater Duct Roughened Artificially With Multiple V-Ribs, *Solar Energy*, *84* (2010), 6, pp.898–911, https://doi.org/10.1016/j.solener.2010.02.004

[18] Gupta, M. K., Kaushik, S. C., Performance Evaluation Of Solar Air Heater Having Expanded

Metal Mesh As Artificial Roughness On Absorber Plate, *International Journal of Thermal Sciences*, *48* (2009), 5, pp.1007–1016, https://doi.org/10.1016/j.ijthermalsci.2008.08.011
[19] Bhushan, B., Singh, R., Nusselt Number And Friction Factor Correlations For Solar Air Heater Duct Having Artificially Roughened Absorber Plate, *Solar Energy*, *85* (2011), 5, pp.1109–1118, https://doi.org/10.1016/j.solener.2011.03.007
[20] Akhtar, N., Mullick, S. C., Approximate Method For Computation Of Glass Cover Temperature And Top Heat-Loss Coefficient Of Solar Collectors With Single Glazing, *Solar Energy*, *66* (1999), 5, pp.349–354, https://doi.org/10.1016/S0038-092X(99)00032-8
[21] Altfeld, K., et. al., Second Law Optimization Of Flat-Plate Solar Air Heaters Part I: The Concept Of Net Exergy Flow And The Modeling Of Solar Air Heaters, *Solar Energy*, *41* (1988), 2, pp.127–132, https://doi.org/10.1016/0038-092X(88)90128-4
[22] Deceased, J. A. D., Beckman, W. A., Solar Engineering Of Thermal Processes. In Design Studies. *3* (1982), 3, https://doi.org/10.1016/0142-694x(82)90016-3
[23] A. Standard. Method Of Testing To Determine Thermal Performance Of Solar Collector. (1977) 93-97.

RECEIVED DATE: 15.4.2024.
DATE OF CORRECTED PAPER: 06.5.2024.
DATE OF ACCEPTED PAPER: 30.8.2024.